43rd Aerospace Sciences Meeting and Exhibit
January 10-13, 2005, Reno, Nevada

AIAA 2005-1371

A Comparative Study Using CFD to Predict Iced Airfoil Aerodynamics

X. Chi*
Department of Mechanical Engineering, Michigan State University
East Lansing, Michigan 48824

Y. Li** **and H. Chen**++**
Exa Corporation
Burlington, Massachusetts 01803

H.E. Addy+ **and Y.K. Choo**+
NASA – Glenn Research Center
Cleveland, Ohio 44135

T. I-P. Shih#
Department of Aerospace Engineering, Iowa State University
Ames, Iowa 50011

WIND, Fluent, and PowerFLOW were used to predict the lift, drag, and moment coefficients of a business-jet airfoil with a rime ice (rough and jagged, but no protruding horns) and with a glaze ice (rough and jagged and has two or more protruding horns) for angles of attack from zero to and after stall. The performance of the following turbulence models were examined by comparing predictions with available experimental data: Spalart-Allmaras (S-A), RNG k-ε, shear-stress transport, v^2-f, and a differential Reynolds stress model with and without non-equilibrium wall functions. For steady RANS simulations, WIND and FLUENT were found to give nearly identical results if the grid about the iced airfoil, the turbulence model, and the order of accuracy of the numerical schemes used are the same. The use of wall functions was found to be acceptable for the rime ice configuration and the flow conditions examined. For rime ice, the S-A model was found to predict accurately until near the stall angle. For glaze ice, the CFD predictions were much less satisfactory for all turbulence models and codes investigated because of the large separated region produced by the horns. For unsteady RANS, WIND and Fluent did not provide better results. PowerFLOW, based on the Lattice Boltzmann method, gave excellent results for the lift coefficient at and near stall for the rime ice, where the flow is inherently unsteady.

1. INTRODUCTION

Ice formation on aircraft wings is a serious safety concern. This is because ice not only reduces lift, but also causes stall to occur at much lower angles of attack.[1] Also, even if the lift is still sufficiently large to sustain flight, uneven ice buildup on the wings can produce flight control problems. Thus, it is critically important to understand the different ice shapes that can form and how they affect aerodynamics.

The effects of ice on aircraft aerodynamics can be studied by flight tests, wind-tunnel measurements, and computational fluid dynamics (CFD) simulations. Of these methods, CFD is the most cost effective. However, the accuracy of its predictions depends on the numerical algorithm, the grid quality and resolution, and the ability of the turbulence model to reproduce the key flow physics.

For iced airfoils – even two-dimensional (2D) ones – the generation of high-quality structured grids is a major

* Graduate Student.
** Research staff.
++ Vice President and Chief Scientist.
+ Aerospace Engineer, Icing Branch. Member AIAA.
# Professor and Chair. Associate Fellow AIAA.

challenge. Chi, et al.[2] presented a number of methods to generate high-quality single- and multi-block structured grids for complicated 2-D ice shapes. Since multi-block grids can converge slower, Zhu, et al.[3] studied the effects of blocking strategy on the convergence rate to steady-state. Zhu, et al.[4] examined the grid-generation and blocking techniques of Chi, et al.[2] and Zhu, et al.[3] by applying them to a much more complicated ice shape, one with multiple, highly extended, and closely packed horns.

Relatively few studies have focused on the effects of turbulence models. Chung, et al.[5,6] used WIND,[7,8] an open source CFD code, to compare the performance of several turbulence models, including the one-equation Spalart-Allmaras (S-A) model[9] and the two-equation shear-stress transport (SST) model.[10,11] They found the SST to perform best with "clean" airfoil (i.e., airfoil without ice) and the S-A model to predict better for an iced airfoil with horns. Chi, et al.[12] studied the effects of turbulence models by using WIND and the popular commercial code, Fluent.[13] With WIND, they examined the S-A model[9] and the SST model.[10,11] With Fluent, they examined S-A,[9] SST,[10,11] standard k-ε,[14] v^2-f,[15,16] and a differential Reynolds stress model (RSM).[17-19] They found WIND and Fluent to give essentially the same results if the grid about the airfoil and the turbulence model used were the same. They also found the S-A model to give better results than the more complicated SST model for iced airfoils. More importantly, they found WIND and Fluent with the S-A model to predict lift and drag with good accuracy until near stall for airfoils with rime ice (i.e., ice shapes that have only roughness and jaggedness but no protruding horns). But WIND with S-A and SST and Fluent with S-A, SST, k-ε, v^2-f, and RSM predicted lift and drag much less satisfactorily for airfoils with glaze ice (i.e., ice shapes with two or more protruding horns near the airfoil's leading edge). However, the conclusions described above were obtained by evaluating only two angles of attack. Also, Chi, et al[12] generated only steady-state solutions so that unsteadiness in the mean flow that may occur near stall or about the horns of glaze ice were not considered.

2. OBJECTIVE

The objective of this study is threefold. The first is to confirm that WIND and Fluent do indeed generate nearly identical results if the grid, the turbulence model used, and the order of accuracy of the numerical schemes used are the same for a range of angle of attacks from zero to and after stall, where the flow can change substantially. This confirmation will allow studies based on WIND to be compared with those based on Fluent on a sound basis. The second is to examine S-A, SST, v2-f, RSM, and a renormalization group (RNG) k-ε model[20,21] for a range of angles of attack for an airfoil with rime ice and with glaze ice, again with and without the use of wall functions. The third objective is to examine the unsteadiness that may exist in the mean flow by performing time-accurate simulations (e.g., unsteady RANS or very large-eddy simulation (VLES)).

Three codes will be used to meet these objectives: WIND, Fluent, and PowerFLOW. WIND and Fluent are based on finite-volume methods that solve the ensemble-averaged Navier-Stokes equations, closed by a turbulence model. Unlike WIND and Fluent, PowerFLOW is based on a method, referred to as the Lattice Boltzmann method[22-26] to solve the Boltzmann equation. The accuracy of CFD predictions will be assessed by comparing computed results with experimentally measured lift, drag and moment coefficients.

The organization of the remainder of this paper is as follows. Section 3 summarizes the glaze and rime, iced-airfoil problems studied. Section 4 outlines the formulation and the numerical method of solution used in the codes and the turbulence models examined. Section 5 presents the results generated. The key results of this study are summarized in Section 6.

3. PROBLEM DESCRIPTION

The airfoil, the ice shapes, and the flow conditions selected for study are those for which the flow field is sufficiently complicated and for which there are experimental data that can be used to assess the accuracy of the CFD predictions. The airfoil selected is the business-jet airfoil (GLC305[1]). The rime ice selected is the 212 ice shape, which has considerable surface jaggedness but no protruding horns. The glaze ice selected is the 944 ice shape with two large protruding horns. The airfoil and the ice shapes about the airfoil's leading edge are shown in Fig. 1 and Fig. 2. See Ref. 1 for details of the geometry.

In this study, the freestream Mach number (M) is 0.12. Two freestream static pressures (P = 20.5 psi and 37.0 psi) and two Reynolds numbers based on the freestream conditions and the chord length (Re = 3.5 x 10^6 and 6.0 x 10^6) are investigated.

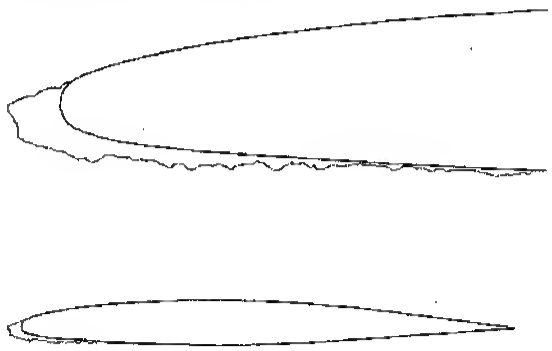

Fig. 1. GLC305 airfoil with 212 rime ice.[1]

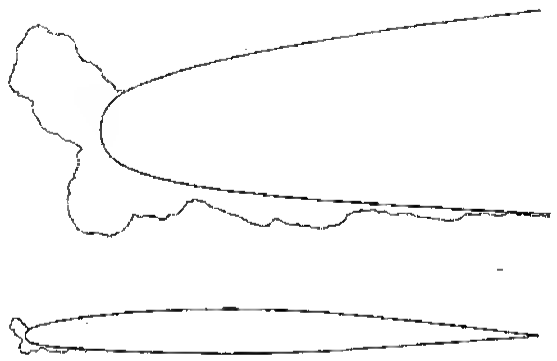

Fig. 2. GLC305 airfoil with 944 glaze ice.[1]

4. FORMULATION AND NUMERICAL METHOD OF SOLUTION

Three different CFD codes were used to generate solutions for the iced-airfoil problems described in the previous section. One is a widely used, open-source code, known as WIND.[7,8] The second code is a popular commercial code, Fluent.[13] The third code is another popular commercial code, PowerFlow,[22,23] which is based on a fundamentally different method. These codes were selected because they are highly versatile and contain a wide range of turbulence models.

WIND and Fluent

For the first two codes, the flow past the GLC305 airfoil with the 944 and 212 ice shape is modeled by the ensemble-averaged conservation equations of mass (continuity), momentum (full compressible Navier-Stokes), and energy for a thermally and calorically perfect gas.

The turbulence models used for simulations of flow past the GLC305 airfoil with the 212 ice shape are as follows. For WIND, the one-equation Spalart-Allmaras (S-A) model[9] was used. For Fluent, S-A turbulence model with and without non-equilibrium wall functions were used.[27-29] More turbulence models were not used for two reasons. First, Chi, et al.[12] has shown that the S-A model gives excellent results for rime ice until near stall. Second, Chung, et al.[5,6] has done an extensive comparative study on turbulence models with WIND. Here, we want to compare predictions from WIND and Fluent in which the grid about the airfoil is the same, the turbulence model is the same, and order of accuracy is the same. If both codes yield identical results, then we can examine results from WIND and Fluent as if they are from the same code.

The turbulence models used for the simulations of flow past the GLC305 airfoil with the 944 ice shape is as follows. For WIND, again, the S-A[9] was used. For Fluent, the following turbulence models were investigated: S-A,[9] SST,[10,11] RNG k-ε [20,21], Durbin's v^2-f model,[15,16] and a differential Reynolds stress model.[17,18,19] With Fluent, the near-wall region is always modeled by enhanced wall treatment, which uses low-Reynolds number models if the grid is sufficiently fine and wall functions if the grid next to the wall is coarse.

The numerical methods of solution used are as follows. For WIND, the convective terms were approximated by second-order Roe upwind differencing. Since only steady-state solutions are of interest, time marching to steady state was accomplished by an implicit method based on ADI-type approximate factorization with local time stepping. For Fluent, which uses a finite-volume method, fluxes at the cell faces are interpolated by using second-order upwind differencing scheme since we found the accuracy of first-order discretization to be very poor although it generally yields better convergence than the second-order scheme. The SIMPLE pressure-velocity coupling algorithm was used to generate steady-state solutions. The convergence criteria used was to require the scaled residuals to be less than 10^{-6} for the energy equation and less than 10^{-3} for all other equations.

A limited number of time-accurate solutions were also generated by using WIND and Fluent. For these unsteady RANS simulations, local-time-stepping were not invoked, and a converged solution was obtained at each time step.

PowerFLOW

For PowerFLOW, the flow field is simulated by using a different set of equations. PowerFLOW does not solve the "macroscopic" Navier-Stokes equations, which are the ones solved in WIND and Fluent. Instead, it uses an extended Boltzmann kinetic approach[24], and solves the "mesoscopic" equations, known as the Lattice Boltzmann equation (LBE), that describes the kinetics of flow particles. The basic hydrodynamic quantities (density, velocity, ...) are obtained through the moment summation of particle density distribution functions[23]. In this approach, sub-grid scale contributions to turbulence are realized through an effective particle relaxation time scale, which can be determined from the renormalization-group based transport equations (revised RNG k-ε sub-grid model)[24]. The LBE based description of turbulent fluctuation carries flow history and upstream information, and contains high order terms to account for the nonlinearity of the Reynolds stress.[22,25] A wall-shear stress model is used to reduce the resolution requirement in the near wall region[22]. The unsteady flow solutions are averaged over a representative time scale to generate mean flow characteristics.

In the numerical implementation, a BGK collision operator with a single relaxation time approximation is used for the Boltzmann equations.[24] The particle density distribution functions are cell centered, and the particle advection is solved by explicit time marching, resulting in

an upwinding scheme (due to the linear advection) with second-order accuracy in space and time.[23,26] The RNG k-ε equations are also solved on the same lattice via a modified Lax-Wendroff-like explicit time marching finite difference scheme[22].

Grid systems for WIND and Fluent

In order to ensure proper comparison between the codes and among the turbulence models, two criteria must be satisfied. The first is that the grid used for each ice shape must be of high quality and provide enough resolution for grid-independent solution. The second is that all codes and turbulence models must use the same grid for each ice shape.

WIND and Fluent used essentially the same grid systems as explained below. For WIND, all grid systems generated consist of two overlapping single-block grids. One is a fine grid next to the airfoil, extending 0.6 chord length from the airfoil in all directions (referred to as the inner grid, as shown in Fig. 3(a)). The other is a coarser grid that overlaps the fine grid by 0.1 chord length and extends 15 chord lengths away from the airfoil in all directions (referred to as outer grid, as shown in Fig. 3(b)). The inner grid is the most important because that is where the flow physics is the most complicated. While generating this grid, grid lines were clustered next to the airfoil surface to resolve the turbulent boundary layer flow. Along the airfoil surface, equal arc-length was employed to create a grid as smooth as possible. The details of the grids used are described later in this section.

Since Fluent cannot handle overlapped grids, the grids used by WIND and by Fluent will not be exactly the same. In this study, Fluent used the WIND's inner grid so that within 0.6 chord length next to the iced airfoil surface, the grids used by WIND and by Fluent are identical. Away from 0.6 chord length, the grids used by WIND and Fluent do differ (contrast Fig. 3 and Fig. 4). Since the most important flow physics about the iced airfoil occur within 0.6 chord length, we do not expect this difference in the grids beyond 0.6 chord length to be important. As results will show, this is indeed the case.

With the above backdrop, the actual grids used for the airfoil with the 212 ice are as follows. For WIND, the outer grid has 125 x 21 grid points, and the inner grid has 987 x 131 grid points (Fig. 5 (a), (b)). For this high quality grid (smooth and nearly orthogonal), the y+ of the first grid point away from the iced airfoil surface is within unity for all angles of attack simulated. Also, the first 5 grid points have y+ values within five. Thus, this is an extremely fine grid. When wall functions are used, the forty grid lines next to the iced airfoil surface were removed so that the first grid point away has a y+ between 30 and 50. For Fluent, the single-block grid used has 987 x 171 grid points, when wall functions are not used. When wall functions are used, the grid has 987 x 140 grid points.

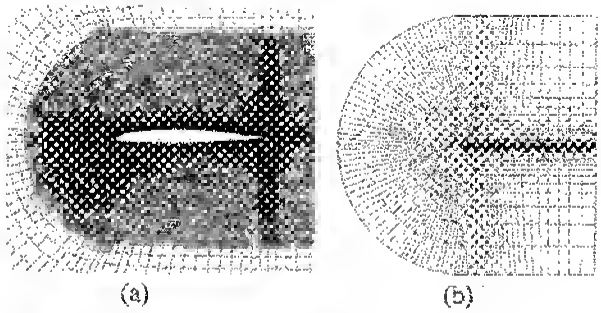

Fig. 3. Grid used by WIND for GLC305 airfoil. (a) Inner grid. (b) Outer grid.

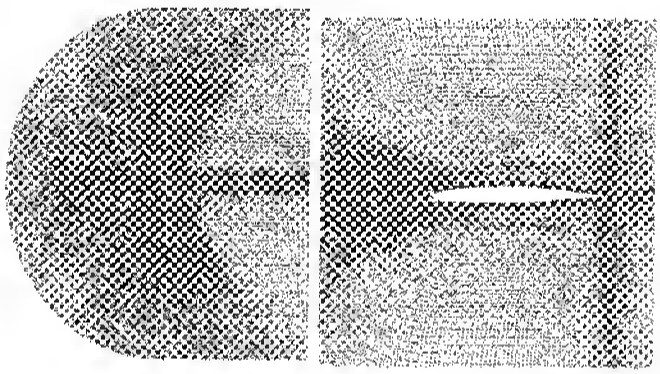

Fig. 4. Grid used by Fluent for GLC305 airfoil with 944 glaze ice.

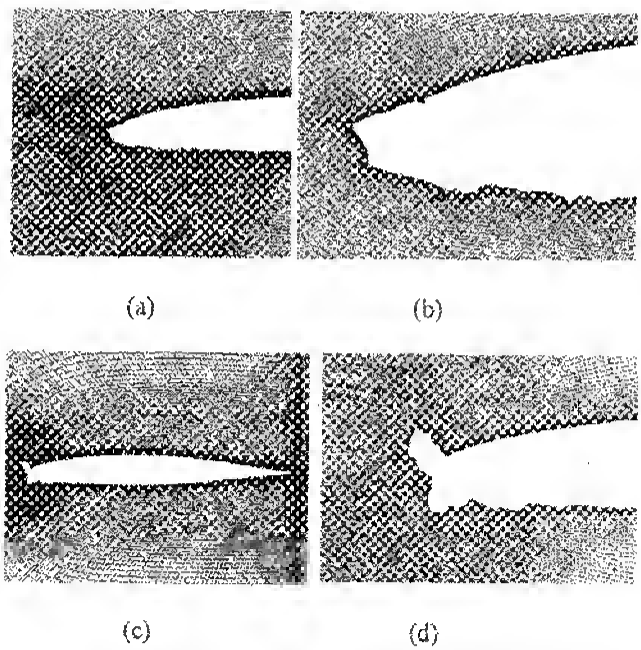

Fig. 5. Grid for GLC 305 airfoil: (a) Inner block grid for 212 rime ice; (b) Close-up of (a); (c) Inner block grid for 944 glaze ice; (d) Close-up of (c).

The actual grids used for the airfoil with the 944 ice are as follows. For WND, the outer grid has 125 x 21 grid points, and the inner grid has 941 x 101 grid points (Fig. 5 (c), (d)). Just like the grid for the 212 ice, the y+ of the first grid point away from the iced airfoil surface is within unity for all angles of attack simulated. Also, the first 5 grid points have y+ values within five. For Fluent, the single-block grid used has 941 x 141 grid points. For the 944 ice, WIND and Fluent did not use wall functions.

The grid systems described above for WIND and Fluent were arrived at after a grid sensitivity study for the RSM model, which is the most stringent on grid requirement. All grids were generated by using transfinite interpolation[30,21] in the manner described in Refs. 2, 3, and 4 with varying degrees of local elliptic smoothing. Gambit was used to generate the outer grid for Fluent.

Grid System for PowerFlow

For PowerFLOW, a Cartesian grid structure is used for the flow simulation. The fluid field is discretized into a set of regular cubic lattice cells and the original CAD geometry (an STL format file for the iced airfoil) is overlaid on the Cartesian mesh to represent the exact fluid/solid interface as shown in Fig. 6 (left). In order to achieve computation efficiency, variable resolution (VR) regions are applied as shown in Fig. 6 (right). Here, each bounding box represents one grid resolution level and VRs cascade outwards from the fine resolution region toward the coarse resolution region. Resolutions differ by a factor of two between two adjacent VR regions[22]. The total number of lattice cells used is 132,042 for the 212 ice and 104,002 for the 944 ice.

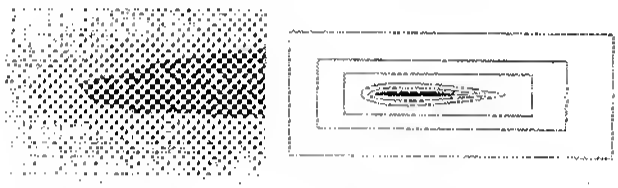

Fig. 6. Cartesian grid method (left) and Variable Resolution regions (right) used in PowerFLOW.

5. RESULTS

The main objective of this study is to assess how well CFD can predict lift, drag, and moment as a function of the angle of attack for a 2D airfoil with a rime ice shape and a glaze ice shape. The focus is on the effects of turbulence modeling and code on the predictions.

Before presenting the results, the abbreviations used in the plots are defined. **Exp** denotes measured experimental data from Ref. 1. **WIND**, **F**, and **LBM** denote results obtained by WIND, Fluent, and PowerFLOW, respectively. **SA**, **SST**, **RNG**, **V2F**, and **RSM** denote Spalart-Allmaras, shear-stress transport, RNG k-ε, v^2-f, and differential Reynolds stress model, respectively. **EW** and **NW** denote enhanced wall treatment and non-equilibrium wall function options in Fluent. If a result is denoted by EW or nothing is said about near-wall treatment, then the finest grids were used to generate that solution and wall functions were not used.

The x-axis of all plots is the angle of attack (**AOA**). Note that every symbol on the plot (e.g., +, triangle, square, ...) indicates a simulation has been done at that angle of attack. The y-axis labels – C_L, C_D, and C_M – denote the lift, drag, and moment coefficients, respectively. The moment coefficient was taken with respect to ¼ chord distance from the leading edge of the clean airfoil.

5.1 CFD Predictions of 212 Rime Ice

WIND versus Fluent

Figures 7 and 8 show results obtained by using WIND and Fluent for the business jet airfoil with the 212 ice for angles of attack from zero to past stall. These figures show that if the grid about the iced airfoil, the turbulence model, and the order of accuracy of the schemes are the same, then WIND and Fluent give nearly identical results for the lift and drag coefficients are nearly at all angles of attack. This means that it is possible to use comparative studies based on WIND and on Fluent to assess turbulence models (i.e., findings based on one CFD code should also apply to another CFD code). This is very comforting for all who work in CFD because the results should be the same if the formulation and the grid are the same. These figures also show that the S-A model provides excellent results until near stall. Both WIND and Fluent under predict the stall angle by about 2 degrees.

S-A versus RNG k-ε with and without Wall Functions

Figures 9 to 11 show the results obtained by using the Fluent code with the S-A and the RNG k-ε models and with different wall treatments. From these figures, it can be seen that for the business-jet airfoil with the 212 ice, S-A and RNG k-ε models give very similar results for the lift, drag, and moment coefficients. Also, it can be seen that the non-equilibrium wall functions can be used with reasonable accuracy. By allowing wall functions to be used, the number of grid points can be markedly reduced and convergence to steady state can be achieved with few iterations.

Thus, the S-A model with wall functions and the RNG k-ε model with and without wall functions perform as well as the S-A model that do not use wall functions. The reason for comparing with the RNG k-ε with wall functions is because PowerFLOW uses wall functions, and only has the RNG k-ε model. This study shows that this model is as good as the S-A model.

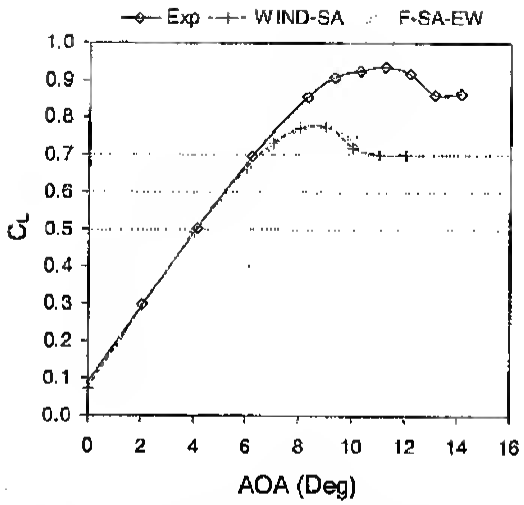

Fig. 7. 212 rime ice: lift coefficient = f (AOA).

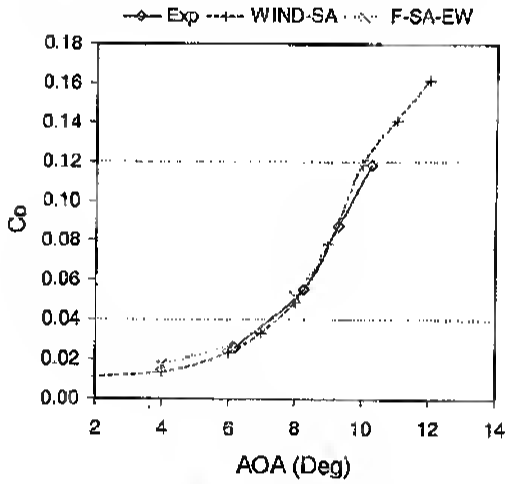

Fig. 8. 212 rime ice: drag coefficient = f (AOA).

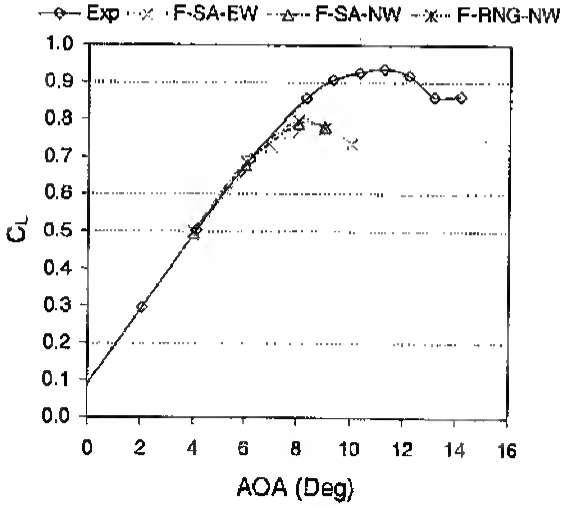

Fig. 9. 212 rime ice: lift coefficient = f (AOA).

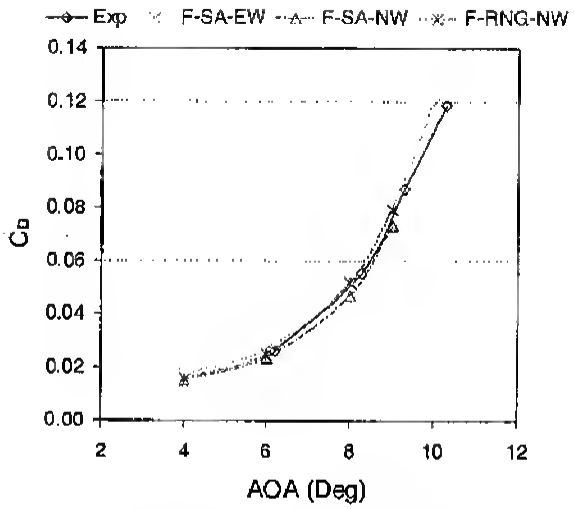

Fig. 10. 212 rime ice: drag coefficient = f (AOA).

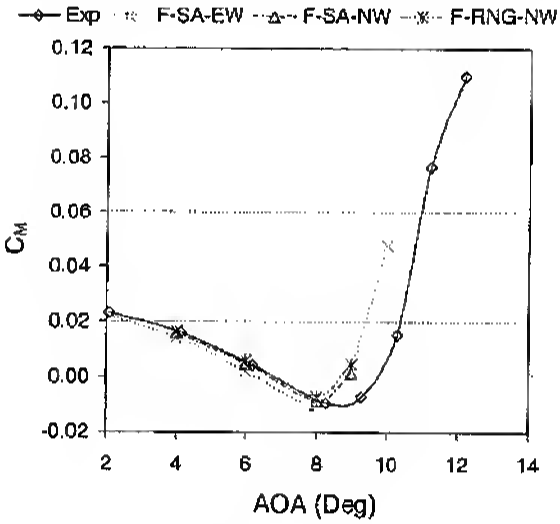

Fig. 11. 212 rime ice: moment coefficient = f (AOA).

Steady RANS versus Unsteady RANS and VLES

For the business-jet airfoil with the 212 ice, WIND and Fluent predict, lift, drag, and moment coefficient quite well at low angles of attack. It is only when the stall angle is approached that lift is under predicted. Since the flow is known to become unsteady as the stall angle is approached because of vortex shedding and unsteady separation, time-accurate solutions may need to be performed; i.e., instead of steady RANS simulations, we need to do unsteady RANS simulations. Efforts were made to perform time-accurate computations with WIND and Fluent. However, for both of these codes, unsteadiness did not appear to be significant. As a result, we wanted to explore other codes that can resolve the unsteadiness with greater fidelity. The code that we found success was the PowerFLOW code, which uses the Lattice Boltzmann method (LBM) to do VLES.

Figures 12 and 13 show how PowerFLOW with RNG k-ε sub-grid model compare with the Fluent RNG k-ε model. Figure 12 shows PowerFLOW to predict the lift coefficient significantly better near stall. It also predicts the stall angle better, within about 1 degree of the experimental data. However, Fig. 13 shows the drag to be predicted with less accuracy when compared to Fluent.

The improvement in the lift prediction might be that PowerFLOW is an unsteady flow solver and is able to capture more flow physics at high AOA via VLES, where flow field is quite unsteady. The difference in the drag prediction maybe due to the fact that the two codes use different models to describe the near wall flow region, which may lead to different surface pressure distributions near the leading edge flow separation region, and the airfoil drag coefficient, is quite sensitive to such a difference in Cp distributions. Further examining of the wall models used in these two approaches are needed.

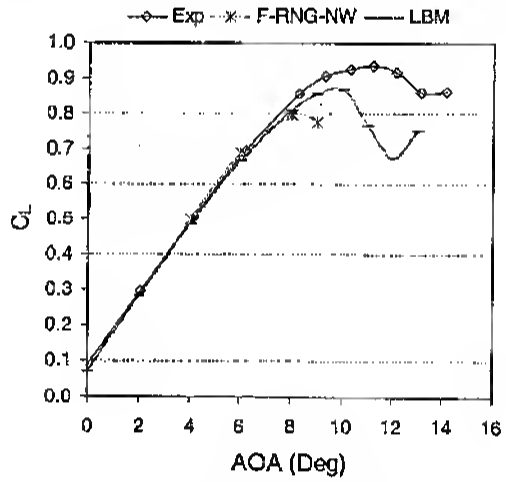

Fig. 12. 212 rime ice: lift coefficient = f (AOA).

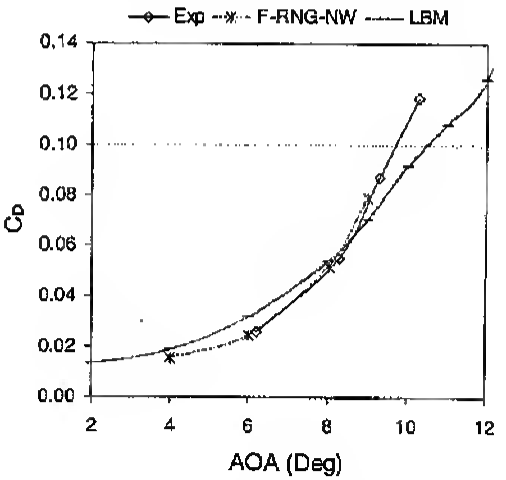

Fig. 13. 212 rime ice: drag coefficient = f (AOA).

WIND vs. Fluent vs. PowerFLOW

Figures 14 and 15 compares all results generated for the business-jet airfoil with the 212 ice by using WIND, Fluent, and PowerFLOW. From Fig. 14, it can be seen that all codes and models examined predict well at low angles of attack. At angles of attack near or after stall, the lift is always under predicted. Only PowerFLOW with LBM predicts lift well near stall.

Figure 15 shows WIND and Fluent to predict drag with reasonable accuracy. PowerFLOW, however, does worse here. Thus, more research is needed here.

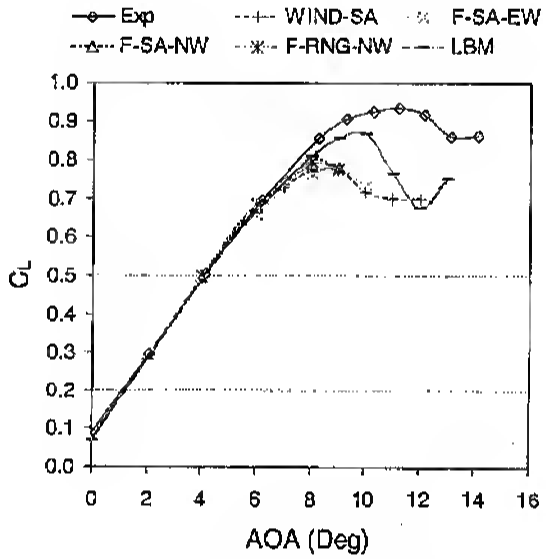

Fig. 14. 212 rime ice: lift coefficient = f (AOA).

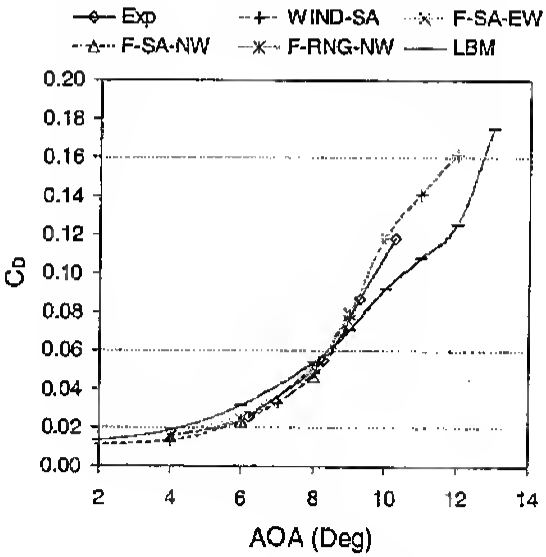

Fig. 15. 212 rime ice: drag coefficient = f (AOA).

5.2 CFD Predictions of the 944 Glaze Ice

So far, we have only examined the capability of CFD in predicting lift, drag, and moment of an airfoil with rime ice, which are ice shapes that have roughness and jaggedness but no protruding horns. In this section, we examine how well CFD can predict the lift, drag, and moment of an airfoil with glaze ice, which has roughness, jaggedness, and large protruding horns. Once there are two or more horns, the flow becomes considerably more complicated. For glaze ice, all simulations performed here by WIND and Fluent did not use wall functions because we wanted to resolve the near-wall region flow features as accurately as possible. With PowerFLOW, however, wall functions are still used.

Similar to our study on rime ice, we want to make sure that for glaze ice, WIND and Fluent will provide the same results if the grid about the iced airfoil, the turbulence model, and the order of accuracy of the schemes used are the same. Figures 16 and 17 show that this is indeed the case.

Figure 16 shows the S-A model to under-predict the lift coefficient even at fairly low angles of attack. This is because when there are horns, large separated regions form even at zero angle of attack. Figure 17 shows the S-A model to under predict drag at all angles of attack. Only the trend is predicted correctly.

Since the S-A model is only a one-equation model, perhaps more advanced models such as SST, RNG k-ε, v^2-f, and RSM can yield better results. Cbi, et al.[12]. did not find this to be the case. But, they only evaluated these models at two angles of attack. In this study, these models are evaluated at angles of attack from zero to after stall. The results generated are shown in Figs. 18 to 20. These figures show that different turbulence models give quite different prediction, which implies turbulence modeling is the key part for further improvement. Figure 18 shows the S-A and the RNG k-ε turbulence models to give the best predictions in the lift coefficient. SST turbulence model is second. Surprisingly, v^2-f and RSM models did not provide satisfactory results on lift.

Figure 19 shows the v^2-f and the RSM models to give the best results on the drag coefficient. While v^2-f model is a little better than the RSM model. S-A, SST, and RNG k-ε models performed poorly.

Figure 20 shows predictions of the moment coefficient. Predictions by v^2-f and RSM turbulence models match experimental data much better than the results by S-A, SST, RNG k-ε turbulence models.

Here, it is noted that for these steady RANS simulations, v^2-f and RSM are very hard to converge. S-A, SST, and RNG k-ε converge relatively easily.

Figure 21 shows time-averaged results from time-accurate simulations performed by using PowerFLOW. From this figure, it can be seen that lift is predicted a little better. Figure 22 shows PowerFLOW to predict drag

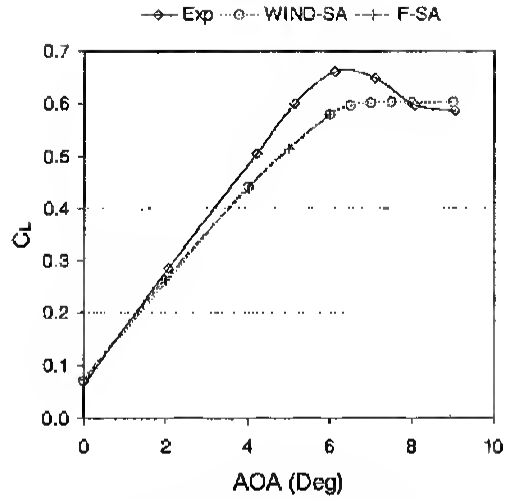

Fig. 16. 944 glaze ice: lift coefficient = f (AOA).

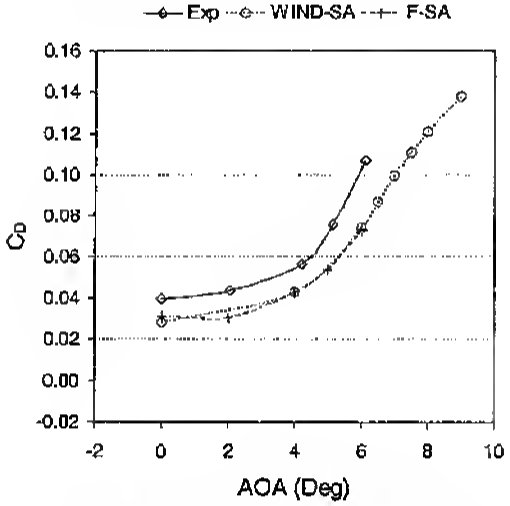

Fig. 17. 944 glaze ice: drag coefficient = f (AOA).

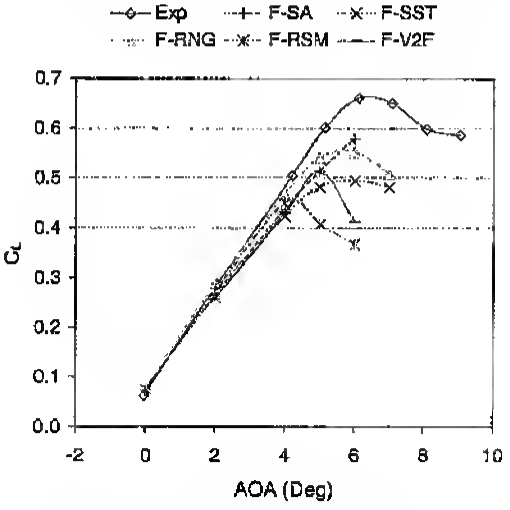

Fig. 18. 944 glaze ice: lift coefficient = f (AOA).

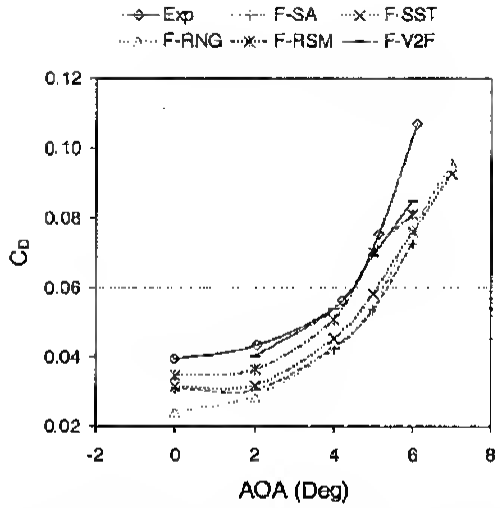

Fig. 19. 944 glaze ice: drag coefficient = f (AOA).

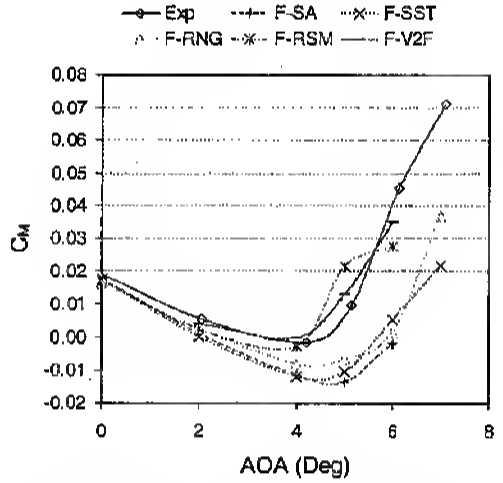

Fig. 20. 944 glaze ice: moment coefficient = f (AOA).

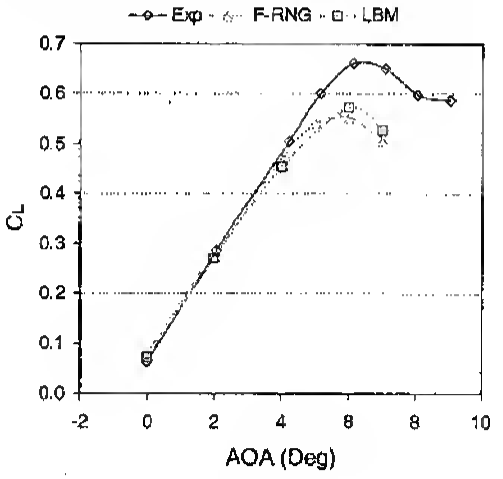

Fig. 21. 944 glaze ice: lift coefficient = f (AOA).

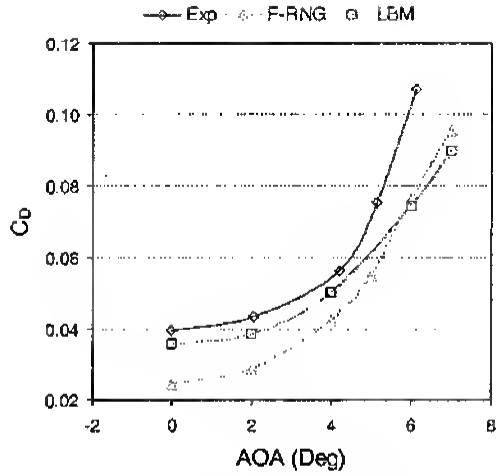

Fig. 22. 944 glaze ice: drag coefficient = f (AOA).

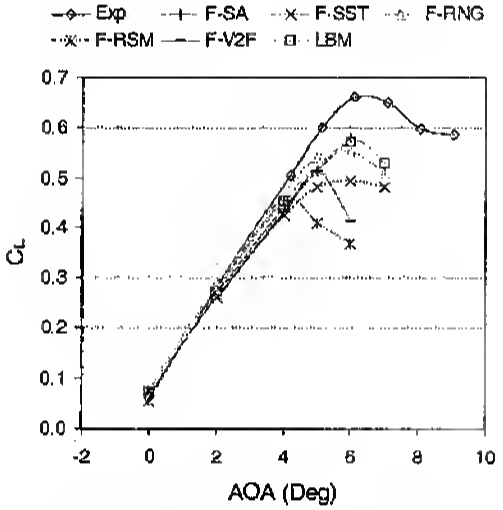

Fig. 23. 944 glaze ice: lift coefficient = f (AOA).

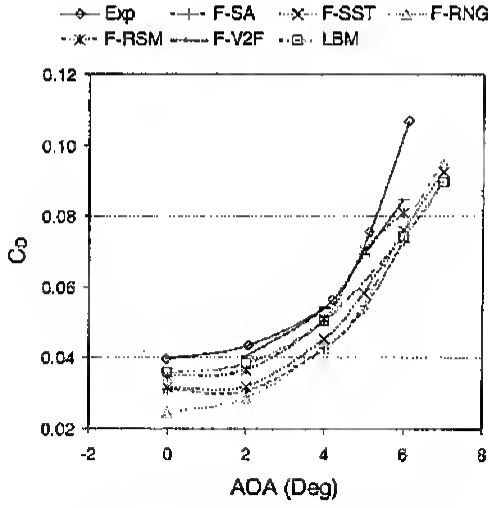

Fig. 24. 944 glaze ice: drag coefficient = f (AOA).

reasonably well at low angles of attack, but slightly worse than S-A at high angles of attack. The inability of PowerFLOW to perform better for glaze ice may be due to its wall function treatment of the near-wall region.

Figures 23 and 24 compares all results generated for the business-jet airfoil with the 944 glaze ice by using Fluent and PowerFLOW. These figures show that PowerFLOW with the LBM method predicts lift better. The v^2-f and the RSM models predict drag better.

6. SUMMARY

For the 212 rime ice and the 944 glaze ice, if the grid used about the iced airfoil, the turbulence model, and the order of accuracy of the numerical schemes used are the same, then the results obtained are essentially identical whether one uses WIND, Fluent, or PowerFLOW. Thus, government and commercial CFD codes are now like LDV and PIV system that you can buy or license, but still must use correctly to get meaningful results.

For the 212 rime ice, WIND, Fluent, and PowerFLOW all gave excellent results for lift except at angles of attack near stall. At angles of attack near and after stall, PowerFLOW gave the best results because the unsteady mean was resolved by VLES. On drag, WIND and Fluent provided excellent agreement with experimental data. If the Reynolds number of the flow is high so that grid lines at y+ of 30 to 50 are still very close to the iced airfoil surface (i.e., the key features of the ice geometry is still resolved by the coarser mesh), then the use of non-equilibrium wall functions were found to yield results similar to those from low Reynolds turbulence models.

For the 944 glaze ice with two large protruding horns in addition to surface roughness and jaggedness, CFD yielded much less satisfactory results. Among the RANS turbulence models, S-A gives the best lift predictions followed by RNG k-ε. v^2-f and RSM give much less satisfactory results on lift, but provide the best drag prediction. PowerFLOW with the LBM gives the best lift prediction by resolving the unsteadiness that may occur, but prediction on drags could be improved. For PowerFLOW, a low Reynolds number near-wall model is needed.

ACKNOWLEDGEMENT

This work was supported by NASA grant NAG 3-2576 and NNC04GB25G from NASA - Glenn Research Center. The authors are grateful for this support. The authors are also grateful to Fluent for providing the Fluent code and to Exa Corporation for providing the PowerFlow code.

REFERENCES

1. Addy, H.E., "Ice Accretions and Icing Effects for Modern Airfoils," NASA/TP-2000-210031, April 2000.
2. Chi, X., Zhu, B., Shih, T.I-P., Slater, J.W., Addy, H.E., and Choo, Y.K., "Computing Aerodynamic Performance of 2D Iced Airfoils: Blocking Topology and Grid Generation," AIAA Paper 2002-0381, January 2002.
3. Zhu, B., Chi, X., Shih, T.I-P., and Slater, J.W., "Computing Aerodynamic Performance of 2D Iced Airfoils: Blocking Strategies and Convergence Rate," AIAA Paper 2002-3049, June 2002.
4. Zhu, B., Chi, X., Shih, T.I-P., Slater, J.W., Addy, H.E., and Choo, Y., "Computing Aerodynamic Performance of 2-D Iced Airfoils with Structured Grids," AIAA Paper 2003-1071, January 2003.
5. Chung, J., Choo, Y., Reehorst, A., Potapczuk, and Slater, J., "Navier-Stokes Analysis of the Flowfield Characteristics of an Ice Contaminated Aircraft Wing," AIAA 99-0375.
6. Chung, J.J. and Addy, H.E., "A Numerical Evaluation of Icing Effects on a Natural Laminar Flow Airfoil," AIAA Paper 2000-0096, Jan. 2000.
7. Mani, M., "A Structured and Hybrid- unstructured Grid Euler and Navier-Stokes Solver for General Geometry," AIAA Paper 2004-0524, Jan. 2004.
8. Nelson, C., Lankford, D., Nichols, R., "Recent Improvements to the WIND(-US) Code at AEDC," AIAA Paper 2004-0527, Jan. 2004.
9. Spalart, P.R. and Allmaras, S.R., "A One-Equation Turbulence Model for Aerodynamic Flows," AIAA Paper 1992-0439, January 1992.
10. Menter, F.R., 1991, "Performance of Popular Turbulence Models for Attached and Separated Adverse Pressure Gradient Flows," AIAA J., Vol. 30, No. 8, pp. 2066-2071.
11. Menter, F.R., 1993, "Zonal Two-Equation k-ω Turbulence Models for Aerodynamic Flows," AIAA Paper 93-2906.
12. Chi, X., Zhu, B., Shih, T.I-P., Addy, H.E., and Choo, Y.K., "CFD Analysis of the Aerodynamics of a Business-Jet Airfoil with Leading-Edge Ice Accretion," AIAA Paper 2004-0560, Aerospace Sciences Meeting, Reno, January 2004
13. http://www.fluent.com/software/fluent/index.htm.
14. Launder, B.E. and Spalding, D.B., "The Numerical Computation of Turbulent Flows," Computer Methods in Applied Mechanics and Engineering, Vol. 3, 1974, pp. 269-289.
15. Durbin, P.A., "Separated Flow Computations with the k-ε-v2 Model," AIAA Journal, pp. 659-664, Vol. 33(4), 1995

16. Durbin, P.A., "A Reynolds Stress Model for Near-Wall Turbulence," Journal of Fluid Mechanics, pp. 465-498, Vol. 249, 1993.
17. Launder, B.E., "Second-Moment Closure: Present... and Future?" International J. Heat Fluid Flow, Vol. 10(4), 1989, pp. 282-300.
18. Fu, S., Launder, B.E., and Leschziner, M.A., "Modeling Strongly Swirling Recirculating Jet Flow with Reynolds-Stress Transport Closures," Sixth Symposium on Turbulent Shear Flows, Toulouse, France, 1987.
19. Gibson, M. M. and Launder, B. E., "Ground Effects on Pressure Fluctuations in the Atmospheric Boundary Layer," J. of Fluid Mechanics, Vol. 86, 1978, pp. 491-511.
20. Yakhot, V. and Orszag S. A. "Renormalization group analysis of turbulence. I. Basic theory," J. Sci. Comput., Vol. 1, pp. 3-51, 1986.
21. Smith, L. M. and Woodruff S. L. , "Renormalization-group analysis of turbulence", Annu. Rev. Fluid. Mech. Vol. 30, pp. 275-310, 1998.
22. Li, Y., Shock, R., Zhang, R., Chen, H., and Shih, T.I-P. "Simulation of Flow over an Iced Airfoil by Using a Lattice-Boltzmann Method," AIAA Paper 2005-1103, January 2005.
23. Chen, S. and Doolen, G. D.,"Lattice Boltzmann Methods for Fluid Flows," "Lattice Boltzmann Method for Fluid Flows," Ann. Rev. Fluid Mech., Vol. 30, 1997, pp. 329-364.
24. Chen, H., Kandasamy, S., Orszag, S., Shock, R. , Succi, S., and Yakhot, V., "Extended Boltzmann kinetic Equation for turhulent flows." Science Vol. 301, 2003, pp. 633-636.
25. Chen, H., Orszag S. Staroselsky I., and Succi S., " Expanded Analogy between Boltzmann Kinetic Theory of Fluid and Turbulence", *J. Fluid Mech.*, Vol. 519, 2004, pp. 307-314.
26. Chen, H., Teixeira, C., and Molvig, K. "Digital physics approach to computational fluid dynamics: some basic theoretical features" Int. J. Mod. Phys. C Vol. 8, 1997, pp. 675-684.
27. Jayatilleke, C., "The Infuence of Prandtl Number and Surface Roughness on the Resistance of the Laminar Suhlayer to Momentum and Heat Transfer," Prog. Heat Mass Transfer, Vol. 1, 1969, pp. 193-321.
28. Kim, S.E. and Choudhury, D., "A Near-Wall Treatment Using Wall Functions Sensitized to Pressure Gradient," ASME FED Vol. 217, Separated and Complex Flows, ASME, 1995.
29. Viegas, J.R., Rubesin, M.W., and Horstman, C.C., "On the Use of Wall Functions as Boundary Conditions for Two-Dimensional Separated Compressihle Flows," AIAA-85-0180, AIAA 23rd Aerospace Sciences Meeting, Reno, Nevada, 1985.
30. Shih, T.I-P., Bailey, R.T., Nguyen, H.L., and Roelke, R.J., "Algebraic Grid Generation for Complex Geometries," International J. for Numerical Methods in Fluids, Vol. 13, 1991, pp. 1-31.
31. Steinthorsson, E., Shih, T.I-P., and Roelke, R.J., "Enhancing Control of Grid Distrihution in Algebraic Grid Generation," International J. for Numerical Methods in Fluids, Vol. 15, 1992, pp. 297-311.